TITLE PAGE

Report Title: **Novel Approaches to High-Efficiency III-V Nitride Heterostructure Emitters for Next-Generation Lighting Applications**

Type of Report:	Annual
Reporting Period Start Date:	October 2003
Reporting Period End Date:	December 2004
Principal Author(s):	Russell D. Dupuis
Date Report was Issued:	January 2005
DOE Award Number:	DE-FC26-03NT41946
Name and Address of Submitting Organization:	Georgia Institute of Technology Atlanta, Georgia 30332
Name, phone number and fax number of preparer:	Russell D. Dupuis 404 385-6094 and 404 385-6096 (Fax)

ABSTRACT

We report research activities and technical progress on the development of high-efficiency long wavelength (λ~540nm) green light emitting diodes which covers the first year of the three-year program "Novel approaches to high-efficiency III-V nitride heterostructure emitters for next-generation lighting applications". The first year activities were focused on the installation, set-up, and use of advanced equipment for the metalorganic chemical vapor deposition growth of III-nitride films and the characterization of these materials (Task 1) and the design, fabrication, testing of nitride LEDs (Task 4). As a progress highlight, we obtained improved quality of ~2μm-thick GaN layers (as measured by the full width at half maximum of the asymmetric (102) X-ray diffraction peak of less than 350 arc-s) and higher *p*-GaN:Mg doping level (free hole carrier higher than 1E18 cm^{-3}). Also in this year, we have developed the growth of InGaN/GaN active layers for long-wavelength green light emitting diodes, specifically, for emission at λ~540nm. The effect of the Column III precursor (for Ga) and the post-growth thermal annealing effect were also studied. Our LED device fabrication process was developed and initially optimized, especially for low-resistance ohmic contacts for *p*-GaN:Mg layers, and blue-green light emitting diode structures were processed and characterized.

TABLE OF CONTENTS

LIST OF GRAPHICAL MATERIALS

INTRODUCTION

While great success has recently been achieved in the development of III-N visible light-emitting diodes (LEDs) and lasers in the blue spectral region (λ~400-480nm), less success has been demonstrated in obtaining high-internal quantum efficiency LEDs emitting in the UV and the green spectral regions, i.e., for light-emitting diodes operating in the wavelength range of λ=280-390nm and 530-560nm. We proposed to develop improved green LEDs in this program that are required for a variety of applications, in particular, for efficient, low-cost solid-state white and colored lighting.

Most blue and green LEDs made today are manufactured from the InAlGaN system while the yellow, orange and red LEDs are made from the InAlGaP system, as shown in Figure 1. The internal quantum efficiency of the best green LEDs is still well below that of the best blue LEDs and the efficiency is even lower for longer wavelengths in the yellow. For example, as Krames has reported that currently, the internal quantum efficiency (IQE, η_{int}) of blue LED materials emitting at λ~460nm is ~60% while the IQE of a green LED emitting at λ~525nm is only ~25%, and only ~10% at λ~545nm. Also, the IQE of typical yellow InAlGaP materials emitting at ~590nm is only about 10%[1]. This performance deficiency is often referred to as "the green gap", as shown in Figure 2. Since the internal quantum efficiency of current red LED InAlGaP materials is estimated to be ~90%[1], there is still much room for the improvement of the performance of longer-wavelength pure green and yellow LEDs. Although the best LED performance has been improving with time, the η_{int} of the best LEDs with longer visible wavelength are still significantly worse than the best blue devices.

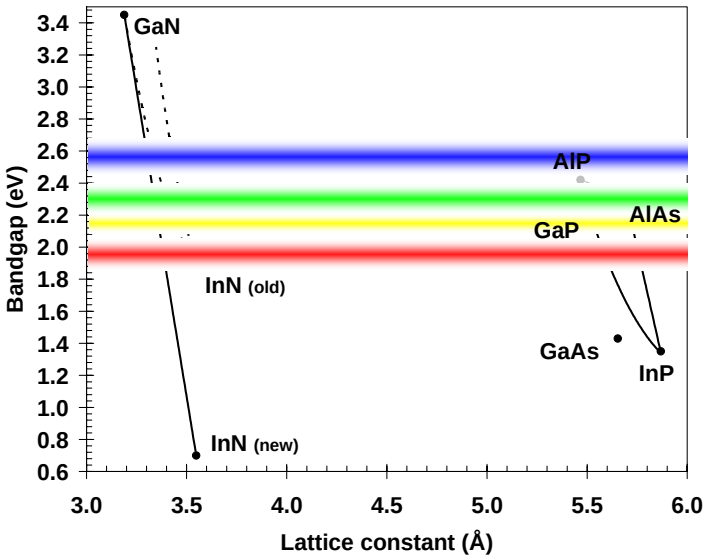

Figure 1: Bandgap energy vs. lattice constant of III-V semiconductor materials for visible light-emitting device applications.

Recently, binary InN single crystals were reported to have a fundamental bandgap energy of 0.65~0.9eV[2] which is dramatically lower than previously reported at 1.89eV (see Figure 1). The recent reports provide new possibilities for InGaN LEDs having green, amber, and red colors with less-than-previously-thought indium composition in the InGaN quantum-well (QW) active layers, indicating less-than-previously-estimated strains.

GaN-based Group III-nitride wide bandgap semiconductor material systems[3] have brought innovative changes in photonic devices, which enable LEDs operating wavelengths to extend into the ultraviolet (UV) spectral region. However, the largest impact to date for III-N LEDs has been from the blue to green visible spectral region which was earlier covered by conventional GaP- and InAlGaP-

based III-V semiconductor material systems. Because no LED device previously covered the blue visible-spectral region, the emergence of III-nitride materials has had an especially tremendous impact on the performance of blue-spectrum LEDs. Adding efficient blue LEDs fills the missing element of the RGB (red-green-blue) primary color elements, which has opened up new opportunities for high-performance solid-state white-light illumination systems[4] and LED-based full-color display systems. Figure 1 shows the bandgap energy of the III-V semiconductor materials that are useful for visible light-emitting device applications. The development of visible LEDs[5] of conventional GaP- or InAlGaP/GaAs-based materials has been focused on pursuing higher luminous performance (lumens/watt), higher quantum efficiency, and shorter operating wavelength. InAlGaP LEDs[6] grown on GaAs substrates, and then wafer-bonded to transparent GaP, have achieved the current record performance in the red and amber (yellow-orange) spectral regime. For example, the external quantum efficiencies (EQE, η_{ex}) were reported to be higher than 50% and luminous performance to be higher than 50lm/W at λ~610nm. The EQE, however, decreases rapidly, as the wavelength decreases (i.e., with more aluminum content in the active layer), especially further into the green spectral regime. The external quantum efficiencies drop to ~9% in the yellow-orange spectral regime (~595nm) and even to ~2% in yellow-green spectral regime (~570nm)[6], due to the loss of one of the carrier (electrons) from the direct Γ band to the indirect X band, governed by the nature of the InAlGaP band structure. Furthermore, InAlGaP materials are not capable of producing blue light emission due to their relatively small bandgap energy.

In contrast to InAlGaP LEDs which have developed from smaller bandgap (red) to wider bandgap (yellow-orange) and which have better performance at smaller bandgap, InGaN LEDs have evolved from the wider bandgap (blue) to smaller bandgap (green). As noted above, IQE is highest in the wavelength of 400~470nm but it decreases rapidly to less than 5% in the wavelength less than 550nm. As a result of the wavelength vs. performance characteristics of InAlGaP and InGaN LEDs, the wavelength regime between 550~580nm remains as a region of "inefficient" LED performance, which is referred to as "the green gap" (Figure 2). Therefore, green LEDs based on InGaN materials have standard of ~525nm peak operating wavelength rather than "true green" 550nm. Decreased efficiency and performance are attributed to excessive strain (hence, quantum confined Stark effect by piezoelectric effect) applied to active layer for green-emitting LEDs. We intend to develop materials growth processes that will provide high-performance InAlGaN LEDs throughout the "green gap".

In this program, we will address the problem of high-efficiency green light emitters using the direct-bandgap InAlGaN quaternary alloy system. Novel epitaxial device structures will be grown using advanced metalorganic chemical vapor deposition (MOCVD) and will be characterized by various structural, optical, electrical characterization techniques, including photoluminescence (PL), cathodoluminescence (CL), time-resolved PL (TRPL), X-ray diffraction (XRD), transmission electron microscopy (TEM), secondary ion mass spectrometry (SIMS), *C-V* profiling, Rutherford back scattering (RBS), and atomic-force microscopy (AFM). Light-emitting devices will be designed, fabricated, and tested to optimize their electrical and optical characteristics.

High-efficiency LEDs are projected to provide a dramatic reduction in the power necessary for industrial and commercial lighting and the full implementation of cost-effective high-performance solid-state lighting is projected by 2025 to reduce the electrical power used world-wide for lighting by over 50%[7]. Furthermore, the development of LED-based lighting

products would, in the USA alone, (1) save 1.66 Quads of electrical energy; (2) reduce the emission of carbon-containing atmospheric waste by 278M metric tons; and (3) generate a cumulative financial savings of $115B over the period 2000-2020[7].

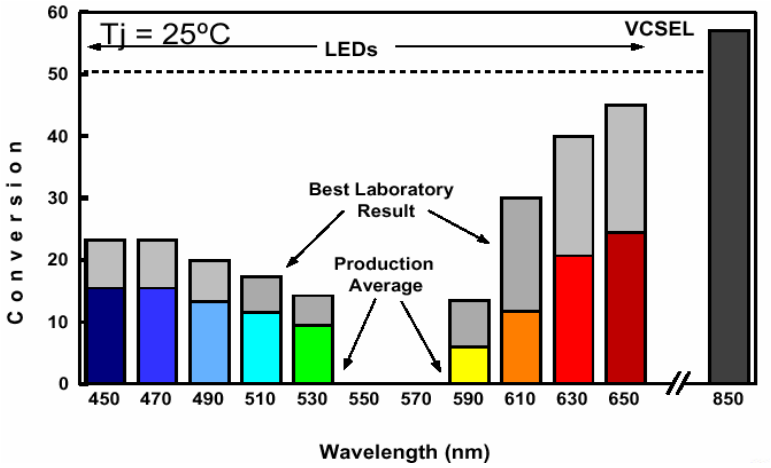

Figure 2: Conversion efficiency vs. wavelength for current generation light-emitting diodes.[8]

In this 36-month project, we are exploring both *INNOVATIVE DEVICE DESIGNS AND MATERAILS GROWTH CONCEPTS*, which will improve the light-emitting capabilities of green LEDs while simultaneously achieving useful optical near-field patterns. These innovative approaches are described in "EXPERIMENTAL" section. The early portion of this program will focus on improved materials growth technologies exploring the use of alternate precursors; the later phases of this program will focus on advanced alternate substrates, e.g., "bulk" GaN and AlN. This work is being performed in collaboration with LumiLeds, a leading USA-based LED manufacturer as an industrial collaborator; a federal research lab, Sandia National Laboratory; as well as a small start-up company that is developing innovative nitride substrates, Crystal IS. Our device approach focuses on several design innovations and unique materials selections, among them are: quantum-dot doping and active regions, strained superlattice barriers, and quantum-dot-quantum-well coupled active regions.

EXECUTIVE SUMMARY

The proposed research program will develop technologies for the growth and fabrication of high-quality green light-emitting devices in the wide-bandgap III-V nitride InAlGaN materials system. This research includes: (1) the use of advanced equipment for the MOCVD growth of III-nitride films and the characterization of these materials; (2) the development of innovative growth technologies for high-quality green light-emitting diodes; (3) the study of strain effects and piezoelectric and polarization effects upon the LED performance; (4) the design, fabrication, testing of nitride LEDs. Our research activities performed in this program during the first year have primarily been focused on Tasks (1) and (4), which will be summarized below:

Since Dupuis' lab moved to new facilities at Georgia Institute of Technology in September 2003, building up of new clean room and lab facilities and moving and installation of major characterization, processing, and measurement equipment for the research were major tasks performed in this period. The activities for the program began with the installation of two new Thomas Swan Scientific Equipment Company Ltd. Close-Coupled Showerhead (CCS) nitride metalorganic chemical vapor deposition (MOCVD) reactors. We have also finished the installation and calibration semiconductor fabrication tools and material structural, optical, and electrical characterization tools, including ICP dry-etching system for the etching of nitride-based devices, susceptor etching system by HCl for the cleaning susceptors used in epitaxial nitride growth, triple-axis XRD system, Hall-effect measurement system, Field-Emission SEM, PL mapping system, CL measurement system, reflectance/transmittance spectrophotometer, electrochemical *C-V* system, contactless sheet-resistance mapping system, and an RTA system. We also have access to other material characterization and processing, such as photolithography, metal evaporation, AFM, etc., located in the clean room of the Georgia Tech Microelectronics Research Center (MiRC). We have set up the electrical device measurement equipment consisting of a probe station with a light-tight enclosure and low-leakage current probes, semiconductor device parameter analyzer, high-power modular device characterization system, high-frequency network analyzer, and Digitizing Signal Analyzer. We have also completed setting up a "quick-test" LED spectral output measurement system. A "quick" LED test set up enables us to approach the optimized growth condition for improved LED performance, such as electroluminescence (EL), *I-V* and *L-I*, more easily by wafer-level testing without device fabrication.

The buffer layer growth technique is one of key technologies that controls the quality of subsequently grown layers of GaN-based materials. We have obtained growth condition for excellent quality ~2μm-thick GaN buffer layers on sapphire substrates exhibiting a narrow line width with a full-width half maximum (FWHM) of low-mid 200 arc-s and low-mid 300 arc-s for (002) and (102) scans, respectively. A cross-sectional TEM study of the buffer layer showed a low total threading dislocation density ~$2x10^8 cm^{-2}$. The *p*-type doping for *p*-GaN and *p*-InGaN were optimized by controlling the dopant activation temperature and time using an RTA as well as the flow rate of the Cp_2Mg with respect to TMGa flow rate and growth temperature and pressure. We achieved GaN:Mg films with p~$1.4E18 cm^{-3}$ and μ=6.3 cm^2/V-s from 300K Hall measurements. We also achieved a much higher doping level (higher than at 5E18) by adding indium (~10% In) to the GaN:Mg layer. This high effective doping level for InGaN (In<0.15) layers can be used to improve the *p*-type contact layers, cladding layers, and current spreading layers of green LEDs.

The essential requirement to achieve GaN-based green LEDs is indium composition control of the InGaN quantum-well active layer material. The incorporation efficiency of indium in the growth of InGaN materials by MOCVD is very sensitive to growth parameters. For the growth of InGaN/GaN MQWs emitting green light, growth parameters such as growth temperature, growth rate, V/III ratio, gallium precursor, quantum well (QW) and quantum well barrier (QWB) transition scheme, etc. were modified to obtain long-wavelength PL emission under controlled growth condition. As expected in general, the PL peak intensity decreases and line width increases, as the peak emission shifts to the longer wavelength side. We achieved PL emission at wavelengths as long as ~540nm, but the active region luminescence quality needs to be further improved to develop a state-of-the-art green LED emitting at ~540nm by further growth parameter optimization. The gallium precursor effect for active layer growth and thermal annealing effects during subsequent layer growth were studied. The PL intensity was brighter for the active regions grown using TEGa compared to TMGa by about a factor of 1.5~2. PL was measured for the sample as-grown and then was measured again after thermal annealing under N_2 atmosphere for about the time expected to be similar to growth time after active region to study the effect of thermal annealing during the growth of subsequent layers on active region luminescence properties. We found that the N_2 atmosphere annealing up to 900C does not degrade the PL quality; instead, it seems helpful to obtain a higher intensity.

The device fabrication process was developed and the electrical properties of *p*- and *n*-contacts and GaN *p*-*n*-junctions were studied to evaluate the basic diode electrical characteristics and device processing development. Diodes had a low turn-on voltage (~3.0V) and series resistance and TLM study showed Ohmic behavior for both *p* and *n* contacts. Both contacts showed a low specific contact resistance, r_c, which are low-E-4 and high-E-4 Ohm·cm^2 for *n*- and *p*- contacts, respectively. Blue-green LEDs were fabricated and characterized, which will be used for reference to the green LED performance characteristics. The devices exhibited electroluminescence of ~406nm and a typical power is ~1.2mW for a 200×200μm^2 device in a unpackaged die form.

As described above, we have primarily performed research on Tasks 1 and 4: (1) the use of advanced equipment for the MOCVD growth of III-nitride films and the characterization of these materials; (4) the design, fabrication, testing of nitride LEDs. In the next year of this program, we will continue the growth of InGaN, AlGaN, and InAlGaN QW structures for green emitters and continue the processing of InAlGaN heterojunction structures and the study of LED device designs. In this second year, we plan to focus as well on Tasks 2 and 3: (2) the development of innovative growth technologies for high-quality green light-emitting diodes; (3) the study of strain effects and piezoelectric and polarization effects upon the LED performance. We will grow green LED structures with improved quantum efficiency based upon research activities that we have carried out during last twelve months.

EXPERIMENTAL

1. MOCVD Growth of InAlGaN Heterostructures for Green Emitters

The InAlGaN heterostructures used in this work were grown by low-pressure MOCVD in a commercially manufactured, specially constructed Thomas Swan Close-Coupled Showerhead (CCS) nitride reactor on two-inch diameter *c*-plane (0001) sapphire, 6H-SiC, or smaller (0001) GaN and AlN substrates. The reactor system is designed to have a capability to accommodate up to seven 2.0 in. diameter wafers in one run. Generally, most of the non-In-containing nitride materials were grown in a H_2 ambient employing the primary precursors trimethylgallium (TMGa), triethylgallium (TEGa), trimethylindium (TMIn), and trimethylaluminum (TMAl) as alkyl sources, and ammonia (NH_3) as the hydride source. Silane (SiH_4) and bis(cyclopentadienyl)-magnesium (Cp_2Mg) were employed as *n*-type and *p*-type dopant precursors, respectively. Layers containing In were typically grown in a N_2 ambient. For the growth of these III-N materials, Dupuis' new laboratory at the Georgia Institute of Technology has two new Thomas Swan CCS 7x2 MOCVD systems dedicated to nitride growth. These systems have the latest technology for the growth of III-N films and have eight or more individual metalorganic sources, e.g., TMGa, TMIn, TEGa, etc., as well as provisions for four hydride sources, e.g., SiH_4, NH_3, etc.

The basic nitride growth technique we employ exploits the advantages of a two-step growth procedure to optimize the optical and electrical characteristics of the materials used to form the LEDs. The first set of operating conditions involved the low-temperature (~550C), growth of a pseudomorphic ~20 nm thick GaN or AlN buffer layer (BL). Then the temperature was ramped to ~1040-1060C for the growth of the GaN layers. For the growth of InGaN active layers, the growth temperature of ~750-900C was employed. *In-situ* monitoring of the reflectivity of the wafer versus time and emissivity-corrected pyrometry by LayTec EpiTT system were employed to monitor growth temperature of the wafer, *in-situ* surface quality, and growth rate of the layers being grown.

In addition to "standard MOCVD growth techniques", using the new nitride MOCVD systems described above, we will explore the growth of InAlGaN quaternaries using a modulated precursor epitaxial growth (MPEG) approach, which involves sequentially exposing the growth surface to a modulated partial pressure of Column III precursors and Column V precursors. This will create an alloy determined by the relative exposures of In, Al, and Ga in separate growth cycles. MPEG-MOCVD can have some advantages for the low-temperature growth of InAlGaN alloys where phase separation is possibly a problem. It also may provide a technique wherein increased In alloy compositions can be reproducibly achieved. This process may also be interesting because the optimal growth conditions for InGaN and AlGaN are dramatically different. Using the MPEG-MOCVD approach, we can expect that the Al, Ga, and In atoms will have a higher mobility at low temperatures, creating a more uniform alloy composition, reduced local strain and concomitant defect density, and smoother surface morphology. Since these low-temperature-grown InAlGaN alloys are a critical element in the demonstration of high-performance ultra-thin QW active regions, the growth rate can be kept small so that the overall device growth time is not strongly impacted by this approach.

2. Material Characterization for Green Emitters

The properties of InAlGaN epitaxial heterostructures grown were investigated by a variety of material characterizations. The structural property of the epitaxial layers was characterized by X-ray diffraction (XRD) and transmission electron microscopy (TEM). XRD was employed to study crystalline qualities of GaN buffer and the layers subsequently grown from symmetric and asymmetric rocking curve scan. The line width of the peak on rocking curve scans closely related to mosaic spreading induced by various component of dislocations. XRD was also employed to study composition, thickness, and interface quality of multi-quantum well (MQW) active layers from triple-axis ω-2θ scans in conjunction with simulation based on X-ray dynamical diffraction. Microscopic structural defects and features, such as total and each component dislocation density quantification, interface quality of MQWs, and possible defects induced by strain, InGaN layer, Mg dopant, etc.. The chemical properties of the layers were characterized by secondary ion mass spectrometry (SIMS) and Rutherford back scattering (RBS). SIMS was employed for dopant and impurity depth profiling. For accurate composition evaluation, RBS can be employed, since it does not require calibration of matrix materials. The optical properties of the structures were characterized by photoluminescence (PL), cathodoluminescence (CL), and time-resolved PL (TRPL). Especially, CL will be used to study the effect of phase separation on optical qualities of the MQWs. The electrical properties of the layers and structures were characterized by Hall measurement, *C-V* profiling, and contactless sheet resistance mapping system. Macroscopic and microscopic surface morphology of the layer is investigated by Nomarski optical microscope and atomic-force microscopy (AFM). Scanning electron microscope was employed to estimate the thickness and feature sizes of the hetero-epitaxial layers and device structures.

3. Device Fabrication Processing and Measurement for Green Emitters

The fabrication process follows three important steps; namely, patterning etch mask, mesa isolation etch, and metallization processes. First, pattern by SiO_2 etch mask using conventional lithography and liftoff, followed by mesa isolation with a SiO_2 etch mask using ICP (inductively-coupled plasma) dry etching was performed. The SiO_2 mask exhibits good selectivity (~10:1) over the layer to be etched, when etching GaN. Once the mesa was defined, metallization step followed, by depositing bottom layer (*n*-GaN) ohmic contact which is Ti/Al/Ti/Au. As the last step, *p*-GaN layer ohmic contacts which can be Pd/Au or Ni/Au were deposited. All metallization processes were done by E-beam evaporation. Contact annealing was performed at 500C for 1minute.

Once fabrication was done, we first characterized the electrical performance using semiconductor parameter analyzer. The quality of ohmic contacts was studied by TLM (transmission line measurement) characterization. Diode *I-V* characteristics were also measured. Electroluminescence (EL) performance characteristics were measured either by a “quick” LED test set up on a epitaxial wafer by using indium dot contacts or by “full” LED testing on processed LEDs.

RESULTS AND DISCUSSION

1. MOCVD Growth of High Quality GaN Layer

The GaN buffer layer growth technique is one of key technologies that controlled the quality of subsequently grown layers of GaN-based materials on (0001) sapphire and 6-H SiC substrates. The growth conditions GaN buffer layer was optimized for excellent quality 2-3μm thick GaN layers grown on sapphire substrates, exhibiting X-ray diffraction peak with narrow line width of FWHM on rocking curve scans. The narrow line width of the peak on symmetric and asymmetric rocking curve scan represents improved buffer layer crystalline quality which is closely related to dislocation density of the buffer layer. Under optimized growth condition, we achieved peak with FWHM of low-mid 200 arc-s and low-mid 300 arc-s for symmetric (002) and asymmetric (102) scans. Figure 3 shows rocking curves of a GaN buffer layer grown on a sapphire substrate, exhibiting 259 arc-s and 310 arc-s for symmetric (002) and asymmetric (102) rocking curve scans, respectively. The buffer layer structural quality was also investigated by TEM for a GaN buffer layer (~3.5μm) grown under similar growth condition. TEM study was performed by; D. Zakharov and Z. Liliental-Weber at Lawrence Berkeley National Laboratory (LBNL). Figure 4 shows cross-sectional TEM image of the buffer layer containing a low total threading dislocation density of ~$2x10^8cm^{-2}$. The dislocation component analysis shows that screw component, mix component, and edge component dislocation densities were $0.0x10^8cm^{-2}$, $1.3x10^8cm^{-2}$, $0.6x10^8cm^{-2}$, respectively. Figure 4 also shows AFM image of a GaN surface grown on a sapphire substrate, exhibiting 0.25nm of RMS roughness for 5x5μm scan.

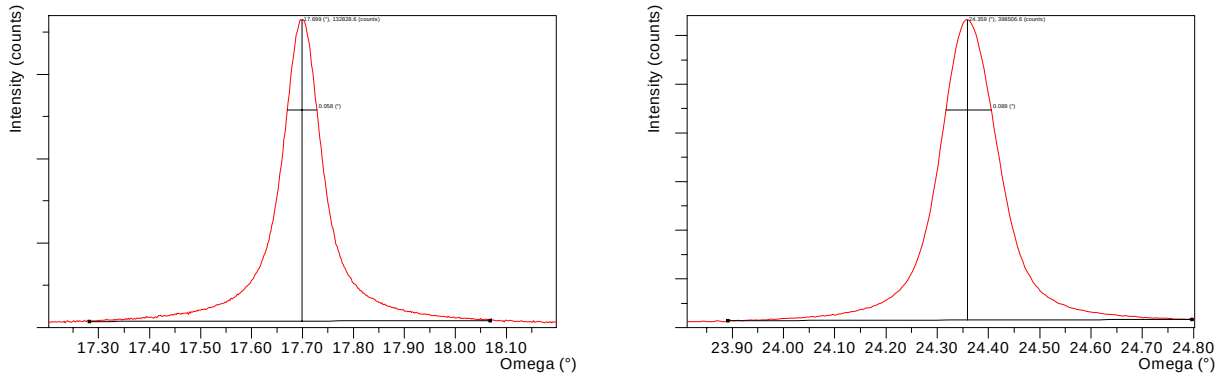

(a) (b)

Figure 3: X-ray rocking curve for ~2 μm thick GaN layer grown on a sapphire substrate, (a) symmetric (002) and (b) asymmetric (102) scans.

The thickness and compositional uniformity is another important parameter for epitaxial growth calibration and the uniformity is affected by the actual growth temperature distribution of the susceptor where the substrate sits and the precursor and shroud flow distribution during the epitaxial growth. We optimized the reactor system parameters to achieve uniform thickness and compositional distribution over the 2" substrate. Figure 5 shows thickness and PL mapping of a GaN layer and InGaN/GaN multi-quantum wells (MQWs). Thickness mapping of a GaN layer shows less than 1.3% of thickness uniformity in terms of standard deviation. The wavelength uniformity of PL peak for InGaN/GaN MQWs, which is affected by both thickness and composition uniformity of MQW shows ~0.6% of uniformity.

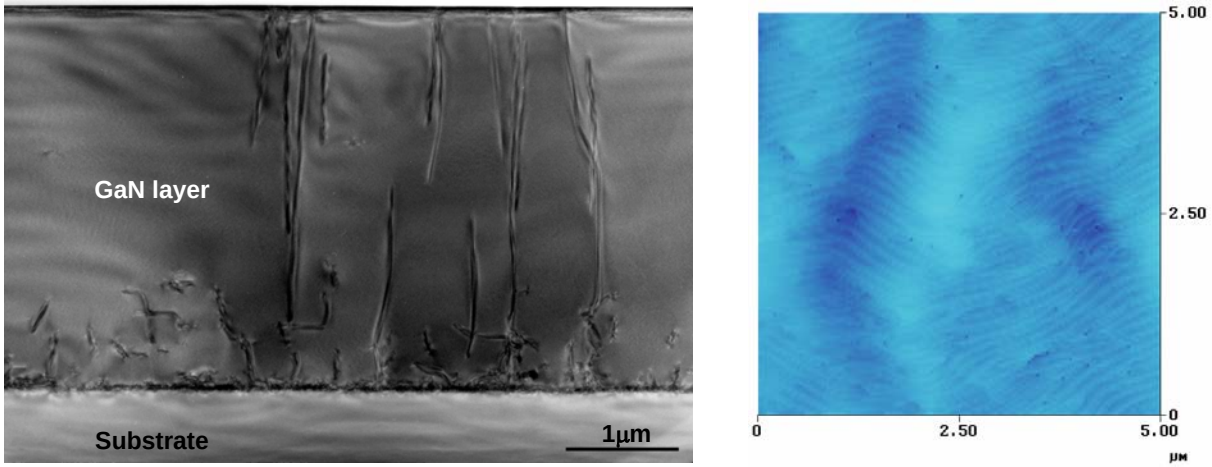

(a) (b)

Figure 4: (a) Cross-sectional TEM image and (b) AFM surface image (5x5µm) of ~3.5 µm thick GaN layer grown on a sapphire substrate.

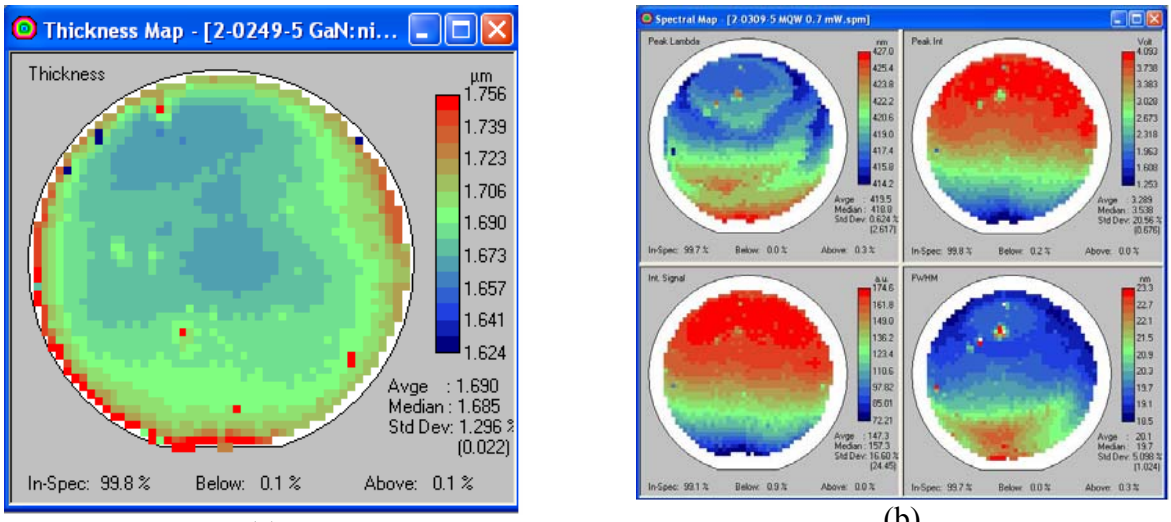

(a) (b)

Figure 5: Thickness and PL mapping showing (a) thickness uniformity of a GaN layer and (b) composition and thickness uniformity of InGaN/GaN multi-quantum wells.

2. p-type and n-type Doping of GaN, InGaN, and AlGaN Layers

Efficient *p*-type doping has been one of the major technical challenges in wide-bandgap semiconductor materials and devices and it still requires intensive optimization process to achieve improved performance devices, especially for improved power conversion efficiency under a given internal quantum efficiency. The *p*-type doping of GaN is known to strongly depend on the material quality of the layer and the background doping level of carbon and oxygen (both can compensate *p*-type doping as donors) as well as Mg incorporation level. The material quality of the layer and oxygen background impurity level is generally well-controlled if the reactor system is well-maintained, while the carbon impurity level and the Mg incorporation efficiency needs to be optimized depending on growth condition.

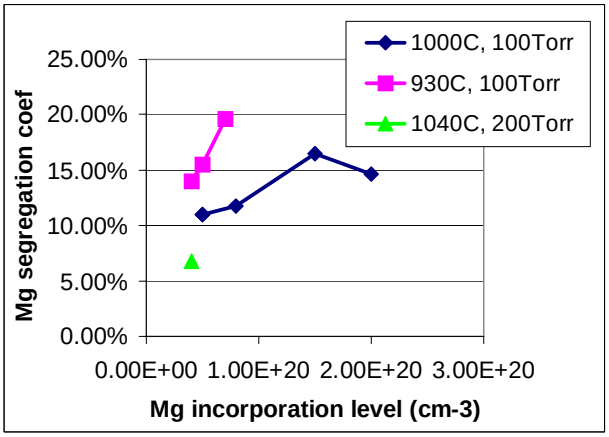

Figure 6: Mg incorporation behavior depending on growth condition.

Systematic investigation of carbon impurity incorporation behavior and Mg dopant incorporation efficiency depending on growth condition was studied. As the growth temperature and pressure increased, the carbon impurity incorporation was reduced. For higher *p*-type doping under a given Mg incorporation level, therefore, a higher growth temperature and pressure is beneficial to minimize the background carbon doping and to obtain better material quality of GaN. However, incorporation of the Mg dopant also depends on growth conditions. Mg dopant incorporation is reduced at higher growth temperature and pressure and growth rate, as shown in Figure 6 (pressure and growth rate effect not shown). Mg segregation coefficient is defined as (Mg incorporation in solid with respect to Ga)/(Mg molar flow rate input in vapor with respect to Ga). As the growth temperature increases from 930 to 1000C at a constant growth pressure, the Mg incorporation efficiency decreases. For controlled *p*-type doping, the growth conditions need to be calibrated to achieve an optimum growth condition of trade-off between the material quality and carbon impurity incorporation and the Mg dopant incorporation efficiency.

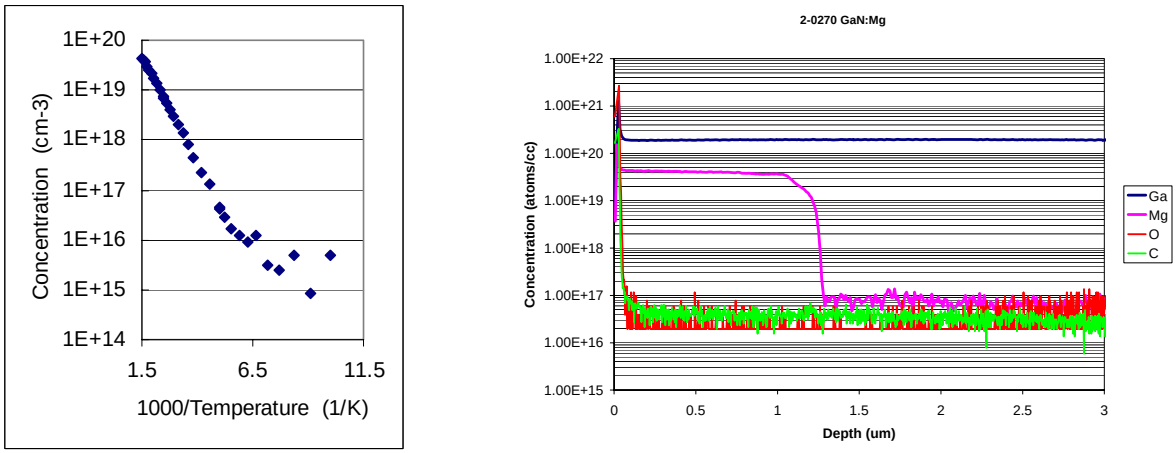

(a) (b)

Figure 7: (a) Temperature-variable Hall measurement and (b) SIMS of *p*-GaN:Mg layer, having free hole concentration, p~1.4E18cm^{-3}.

Under optimized growth conditions for efficient *p*-GaN layers, we achieved a free-hole concentration, p~1.4E18cm^{-3} with a mobility, μ_h~6.3cm^2/V-s at 300K. The resistivity of the layer, ρ was 0.73 Ω-cm. Figure 7 shows the temperature (1000/T) vs. free-carrier concentration plot determined by variable temperature Hall measurement and SIMS depth profiling for the sample exhibiting a free-hole concentration, p~1E18cm^{-3}. Carbon and oxygen impurity levels are well controlled (very low near detection limit) and Mg incorporation into the GaN solid is

4E19cm^{-3}, indicating that ~2.5% of the Mg incorporated into GaN is activated as a *p*-type dopant. From the gradient of temperature (1000/T) vs. free-carrier concentration plot, ~170meV of activation energy was obtained, which is close to the value reported for GaN:Mg activation for *p*-type doping.

Doping calibration for InGaN (In=0.1~0.15) layers was also carried out by changing growth and *ex-situ* annealing condition. We can achieve a much higher doping level by adding indium to GaN. While the free hole concentration strongly depends on the indium composition, growth temperature, Mg incorporation ratio, etc. it was not difficult to obtain a higher than 1E18cm^{-3} of *p*-type doping level. The highest doping level achieved was 5E18cm^{-3} for an InGaN (In~0.1) layer. This is attributed to a decreased activation energy of Mg dopant. Kimkura, et al., reported that the activation energies of *p*-InGaN:Mg are 14, 98, 82 meV for the materials containing In~0.04, In~0.1, In~0.14, respectively[9]. This high doping level of InGaN (In<0.15) layer can be used contact layer, cladding layer, and current spreading layer of green LEDs.

The *n*-type doping of GaN was also calibrated in terms of the doping level and doping uniformity. SIMS depth profiling showed that the carbon and oxygen impurity levels are well controlled for the samples. The sheet resistance was measured to study the doping uniformity of a GaN:Si layer. A 2.5% sheet resistance uniformity (103~112Ω/□ over the 2" wafer) was achieved for the sample showing free electron concentration, n~1.9E18cm^{-3} with μ_e~299cm^2/ V-s from 300K Hall measurement.

An AlGaN layer is used as an "electron blocking" layer for LED structures. We investigated AlGaN layer growth conditions and compositional controllability for the AlGaN electron blocking layer (EBL). AlGaN layers (Al~0.28, 0.37, 0.45, and 0.55) grown for Al composition calibration were characterized by optical measurements to verify the material quality of the AlGaN layers. Sharp optical transmission cut-off and narrow (FWHM ~8 nm) room-temperature PL spectra were obtained. Also notable is the fact that the transmittance cut-off aligns very well with the PL peak wavelength, establishing that the PL is from the band-edge and also indicating the absence of near-bandgap optically active defect states. Impurity levels of AlGaN:Si (Al~0.45) layers were measured by SIMS. These AlGaN layers contained a low concentration of oxygen (low E17) and carbon (low E16), verifying the low level of impurities of the layers, which is critical in *n*-type and *p*-type doping control. A microscopic morphology study by AFM exhibited clear atomic steps with a very smooth surface (<1nm RMS roughness) from AlGaN (Al~0.55) layers. AlGaN EBL requires *p*-type doping by Mg. However, the active free-carrier measurement by Hall measurement is not very practical due to the challenging requirements for Ohmic contacts and of the thick layer growth for the Hall sample. The electrical properties of the layer can be determined from the electrical characteristics of the LED structure with the aid of possible Mg and impurity incorporation level of the electron blocking layer. SIMS analysis of an AlGaN:Mg (Al~0.55) layer having different Mg precursor flow rates was performed for reference of the Mg incorporation of the electron blocking layer. The Mg segregation coefficient can be estimated from the relationship between the precursor flow rate and the Mg concentration in solid.

3. Growth of InGaN/GaN Muti-Quantum Well Active Regions

The essential requirement to achieve GaN-based green LEDs is indium composition control of the InGaN quantum-well active layer material. The incorporation efficiency of indium in the growth of InGaN materials by MOCVD is very sensitive to growth parameters. For the

calibration of the indium incorporation efficiency and InGaN layer compositions, 50~200nm thick InGaN layers were grown on a ~2μm GaN layer. The InGaN layers were characterized by triple-axis XRD and PL. InGaN/GaN MQWs were grown using indium incorporation efficiency data calibrated from bulk InGaN growth for "blue: and "green"-light-emitting layers. We observed X-ray diffraction showing well-developed superlattice-related fringes and TEM images showing clear interface contrast, indicating excellent quality interfaces.

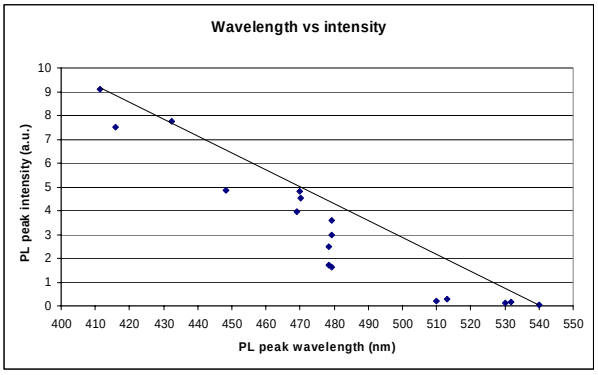

Figure 8: PL intensity change with peak wavelength increase from InGaN/GaN MQWs.

For the growth of InGaN/GaN MQWs emitting green light, growth parameters such as growth temperature, growth rate, V/III ratio, gallium precursor, quantum well (QW) and quantum well barrier (QWB) transition scheme, etc. were modified. We achieved long wavelength PL emission under controlled growth condition. As expected in general, PL peak intensity decreases and line width increases, as peak emission shifts to longer wavelength side, as shown in Figure 8. We have achieved PL emission at as long wavelength as ~540nm, but the active region luminescence quality need to be further improved to develop the-state-of-the-art green LED emitting at ~540nm by further growth parameter optimization.

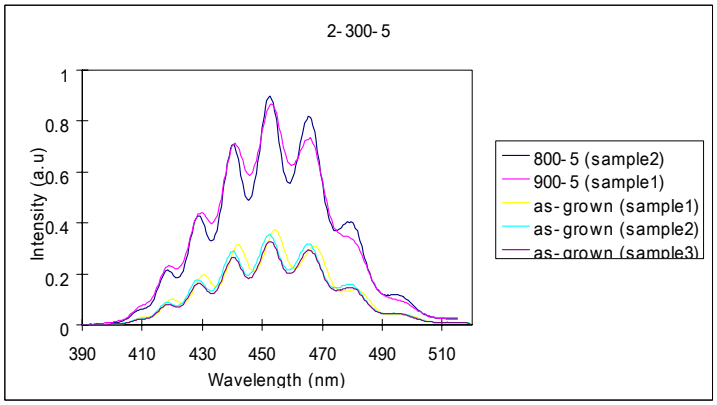

Figure 9: PL intensity change with thermal annealing in N_2 atmosphere for InGaN/GaN MQWs.

The gallium precursor effect [10] for active layer growth and thermal annealing effect during subsequent layer growth were studied. For the comparison of luminescence quality of active region grown by different gallium precursors, TEGa and TMGa, the samples having PL peak at ~450nm and ~520nm ware selected. PL intensity was brighter for the active regions grown by TEGa than by TMGa by about factor of 1.5~2. The green LED MQW active region is generally grown at lower temperature than their nitride-based companions emitting at shorter wavelengths such as blue and violet visible LEDs. For LED structure growth, the GaN *p*-cladding layer needs to be incorporated in the epitaxial structure, which will require a higher growth temperature than the active region. The effect of thermal annealing during the growth of subsequent layers on active region luminescence properties was studied. The PL was measured for the sample as-grown and then was measured again after thermal annealing under a N_2 atmosphere for about the time expected to be similar to growth time after the active region. We have performed, as of report time, to 900C annealing temperature and plan to extend the temperature range to 1050C and

atmosphere with H_2. We found that annealing up to 900C in a N_2 atmosphere does not make the PL quality degrade; instead, it seems to be helpful to obtain a higher intensity, as shown in Figure 9.

4. LED Device Fabrication and Characterizations

Ohmic contact formation, which is one of the important processing steps for all carrier injection devices, was studied and evaluated by TLM. TLM studies of *n*-type GaN:Si layers were performed after ICP etching for mesa formation, since the *n*-contact is formed on an etched surface of mesa structure. The contact was made by Ti/Al/Ti/Au metallization without annealing. The contact shows ohmic behavior and specific contact resistance, r_c, is ~1.9E-4 Ohm·cm^2, as shown in Figure 10. The structure used for the experiments consists of (in the order from the bottom to the top) GaN:nid layer, *n*-type GaN:Si layer (~1.8μm), and *p*-type GaN:Mg layer (~385nm) grown on *c*-plane sapphire substrates. Figure 10 also shows a TLM study on *p*-GaN:Mg layer. A Pd/Au or Ni/Au metallization scheme was employed for contact and specific high doping scheme contact layer is not included in the structure. The specific contact resistance, r_c, of the sample shows 6.0E-4 Ohm·cm^2. Even without a contact layer, the contact of the sample exhibits reasonably good ohmic behavior.

Further improvement of *n*-type ohmic contacts for LED structures was made. The study requires both doping level optimization on the material growth side and ohmic contact device processing optimization on device fabrication side. The *n*-type doping level is well-calibrated and *n*-type ohmic contact showed reasonably low contact resistance using Ti. Here, the Ohmic contacts using V instead of Ti was optimized and AlGaN:Si (Al=0.45~0.55) was chosen for material for a contact layer, since AlGaN growth is more challenging than GaN. This enables us to tell the differences between a contact using Ti and V more effectively. According to the TLM study of the *n*-type contact using different metallization schemes and annealing conditions, both show perfect ohmic behavior but the contact resistance, r_c decreases by the order of magnitude. The contact resistance are 2.0E-3 Ohm·cm^2 and 1.3E-4 Ohm·cm^2 for Ti/Al/Ti/Au and V/Al/Ti/Au, respectively. This *n*-type ohmic contact study can be applied to GaN *n*-type contact ohmic contact for green LEDs to improved further ohmic contact for *n*-type.

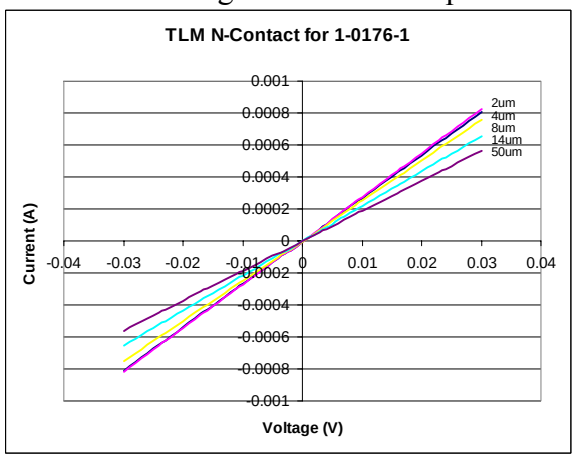

(a)

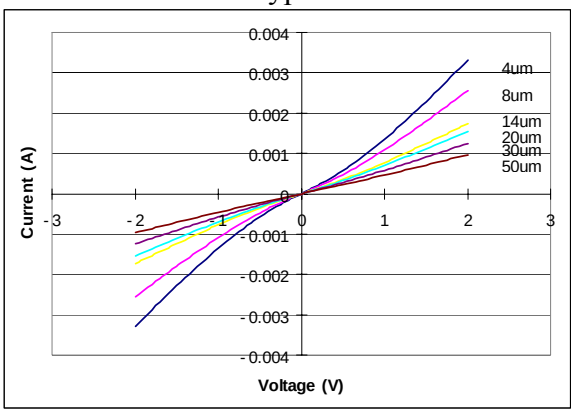

(b)

Figure 10: TLM of (a) *n*-contact on GaN:Si by Ti/Al/Pt/Au metallization and (b) *p*-contact on GaN:Mg by Ni/Au metallization.

GaN *p*-*n*-junctions were grown and fabricated to evaluate basic diode electrical characteristics and for device processing development. The diodes had low turn-on voltages (~3.0V) and series resistance and the TLM study showed Ohmic contact behavior for both *p* and *n* contacts.

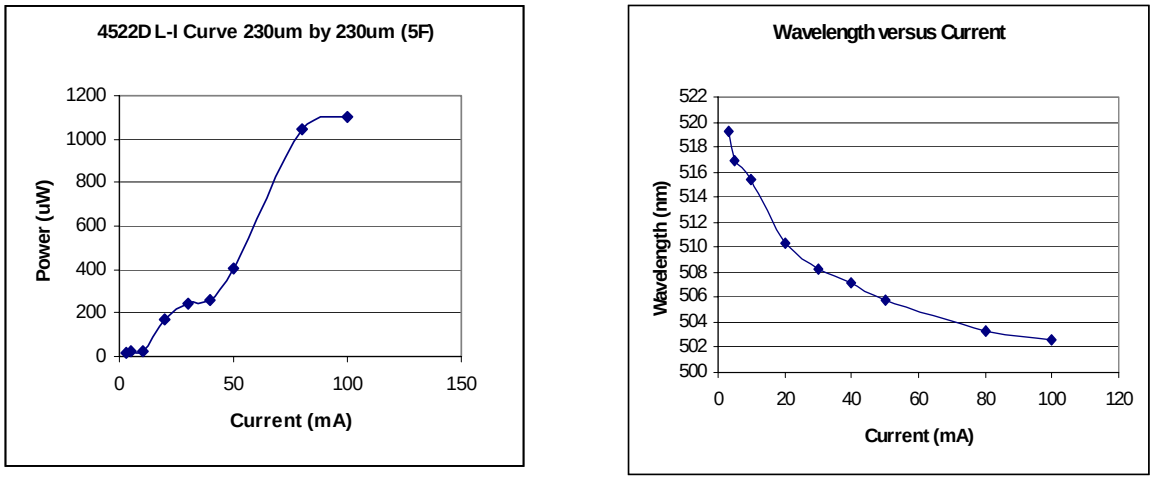

(a) (b)

Figure 11: Electroluminescence of a blue-green LED structure: (a) optical power change vs. current and (b) peak wavelength vs. current.

We have fabricated and characterized blue-green LEDs, which will be used for reference to the green LED performance characteristics. The device structure and fabrication were not highly optimized at this time. For measurements, we have performed wafer-level quick-test mapping as well as the measurement of fully processed devices (unpackaged die form). The devices exhibited electroluminescent of ~406nm and typical power is ~1.2mW for 200×200μm^2 device, as shown in Figure 11. V_f of devices had as low as ~2.84V. Quantum efficiency (IQE) will be estimated.

CONCLUSION

The proposed research program will develop technologies for the growth and fabrication of high-quality, high-efficiency green LEDs in the wide-bandgap III-V nitride InAlGaN materials system. This research includes four Tasks: (1) the use of advanced equipment for the MOCVD growth of III-nitride films and the characterization of these materials; (2) the development of innovative growth technologies for high-quality green light-emitting diodes; (3) the study of strain effects and piezoelectric and polarization effects upon the LED performance; (4) the design, fabrication, testing of nitride LEDs. We report here our technical progress for the first year of this program. We have primarily focused on research on Tasks 1 and 4: (1) the use of advanced equipment for the MOCVD growth of III-nitride films and the characterization of these materials; (4) the design, fabrication, testing of nitride LEDs. We have achieved successful calibration and improved performance and/or qualities for each component of the green LED device structure: (1) improved crystalline quality of GaN buffer layer on sapphire substrates which will serve as a growth template for green LEDs; (2) improved doping level control and

ohmic contact scheme, especially for *p*-GaN:Mg layer for improved carrier injection efficiency; (3) calibration for InGaN/GaN active region to obtain green light emission with improved optical quality and precursor comparison for active region; (4) fabrication process optimization for improved device performance; (5) demonstration of blue-green LEDs; etc.. These improvements in LED structure components will lead us to high-efficiency green LEDs operation emitting at λ~540nm.

While we have taken rather "conventional" approaches to achieve high efficient green LEDs to establish a baseline, in the next year of this program, we will continue the growth of InGaN, AlGaN, and InAlGaN QW structures for green emitters and continue the processing of InAlGaN heterojunction structures and the study of LED device designs with "less-conventional more innovative" approaches. In this second year, we also plan to focus as well on Tasks 2 and 3: (2) the development of innovative growth technologies for high-quality green light-emitting diodes; (3) the study of strain effects and piezoelectric and polarization effects upon the LED performance. We will grow green LED structures with improved quantum efficiency based upon research activities that we have carried out during last twelve months.

LIST OF ACRONYMS AND ABBREBIATIONS

AFM	Atomic force microscopy
arc-s	arc-second
CCS	Close-coupled showerhead
CL	Cathodoluminescence
(Cp_2Mg)	Bis(cyclopentadienyl)-magnesium
C-V	Capacitance-Voltage
E-beam	Electron beam
EBL	Electron blocking layer
EL	Electroluminescence
EQE	External quantum efficiency
ICP	Inductively-coupled plasma
IQE	Internal quantum efficiency
I-V	Current-Voltage
FWHM	Full-width at half maximum
LED	Light emitting diode
L-I	Light-Current
MiRC	Microelectronics Research Center
MPEG	Modulated precursor epitaxial growth
MOCVD	Metalorganic chemical vapor deposition
MQW	Multi-quantum well
PL	Photoluminescence
QW	Quantum well
QWB	Quantum well barrier
RBS	Rutherford back scattering
RTA	Rapid thermal annealing
SEM	Scanning electron microscopy (or microscope)
SIMS	Secondary ion mass spectroscopy
TEGa	Triethylgallium
TMAl	Trimethylaluminum
TMGa	Trimethylgallium
TMIn	Trimethylindium
TEM	Transmission electron microscopy (or microscope)
TLM	Transmission line measurement
TRPL	Time-resolved photoluminescence
UV	Ultraviolet
XRD	X-ray diffraction (or diffractometer)

REFERENCES

[1] M. Krames, DoE Workshop on Solid State Lighting, 2003.

[2] T. Matsuoka, H. Okamoto, M. Nakao, H. Harima, and E. Kurimoto, "Optical bandgap energy of wurtzite InN," App. Phys. Lett. **81**, 1246 (2002).

[3] Group III Nitride Semiconductor Compounds, edited by B. Gil, Oxford University Press, Oxford UK (1998).

[4] S. Muthu, F. J. P. Schurman, and M. D. Pashley, "Red, green, and blue LEDs for white light illumination," IEEE J. Select. Topic Quantum Electron. **8**, 333 (2002).

[5] M. G. Craford, "LEDs challenge the incandescents, IEEE Circuit and Device Mag. **8**, 24 (1992).

[6] D. A. Vanderwater, I. H. Tan, G. E. Hofler, D. C. Defevere, and F. A. Kish, "High-brightness InAlGaP light emitting diodes," Proc. IEEE **85**, 1752 (1997).

[7] "*The Promise of Solid State Lighting for General Illumination—2002 Update*," DoE BTS and OIDA (Published by OIDA, Washington DC, 2002).

[8] This diagram is obtained from the LumiLeds website, http://www.lumileds.com/pdfs/techpaperspres/SPIE2001.PDF.

[9] K. Kumakura, T. Makimoto, N. Kobayashi, "Activation energy and electrical activity of Mg in $In_xGa_{1-x}N$:Mg ($x<0.2$)," Jpn. J. App. Phys. **39**, L337 (2000).

[10] W. Lee, J. Limb, J. H. Ryou, D. Yoo, T. Chung, and R. D. Dupuis, "Effect of gallium precursor on InGaN/GaN multi-quantum-wells and Mg-doped layer for green LEDs," Electronic Materials Conference 2005 (submitted).